

Numerical Analysis of Dielectric Post-Wall Waveguides and Its Application to Realization of Bandpass Filters from Millimeter to THz Waves

Vakhtang Jandieri*⁽¹⁾, Daniel Erni⁽¹⁾, Douglas H. Werner⁽²⁾ and Kiyotoshi Yasumoto⁽³⁾

(1) General and Theoretical Electrical Engineering (ATE), Faculty of Engineering, University of Duisburg-Essen, 47048 Duisburg, Germany

(2) Department of Electrical Engineering, The Pennsylvania State University, University Park, PA 16802, USA

(3) Faculty of Information Science and Electrical Engineering, Kyushu University, Fukuoka 819-0395, Japan

Abstract

A functional dielectric Post-Wall Waveguide (PWW) and a PWW-based bandpass filter that is formed by introducing specific arrangements of additional dielectric posts in the guiding region are analyzed. The complex wavenumber of the dielectric PWW composed of dielectric rods as wall elements is rigorously calculated using our original highly efficient full-wave formalism. Structural parameters of the dielectric PWW are properly chosen using a combination of our method and a breeder genetic algorithm to achieve a strong confinement of electromagnetic fields with a relatively smaller number of layers in the lateral direction aiming at a realization of a compact functional device. A functional bandpass filter is realized and its S-parameters are calculated using the CST 3D-EM simulation tool.

1 Formulation of the Problem

An alternative to the conventional non-planar guiding devices is the PWW [1]. A transversal view of a typical configuration of the PWW is shown in Fig. 1. The electromagnetic fields of the PWW are confined in the lateral direction by periodic arrays of posts placed on both sides of the guiding channel. The height of the waveguide is bounded by two metallic plates and it is much smaller than the excitation wavelength. In our recent manuscript [2], we have shown that in the case of perfect electric conductor (PEC) rods, a single array at both sides of the channel is usually enough to provide strong field confinement and leakage of the guided waves is suppressed by the cutoff phenomenon between the adjacent PEC rods. However, at higher frequencies the metals become increasingly lossy and the dielectric materials start to play an important role. Furthermore, 3-D printers allow a cheap and rapid prototyping by additive manufacturing of plastic materials, which has attracted the interest of engineers for all-dielectric waveguide structures and integration schemes.

A phenomenon of field confinement in the guiding region in the case of dielectric rods is still an open research issue as the wall's elements are completely different from that of PEC rods. In the case of dielectric rods, the confinement is achieved through the electromagnetic band-gap behavior

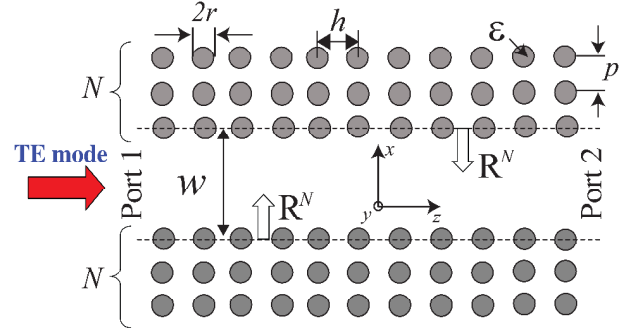


Figure 1. Transversal view of a dielectric PWW, where h is the period of the structure, w is the width of the waveguide, r is the radius of the dielectric rod, p is the distance between the layers, ϵ is the relative dielectric permittivity of the rod, $R^N(k_{z0})$ represents a generalized reflection matrix of the N -layered periodic structure, where k_{z0} is the complex wavenumber. Guidance of a fundamental TE mode (E_y , H_x , H_z) injected in the dielectric PWW through Port 1 is considered.

similar to Bragg reflection in a periodic multilayered structure along the x -axis (see Fig. 1). As a result, good confinement of the field can be achieved at the expense of a larger transversal extent of the device.

In this work, we numerically analyze a PWW composed of periodically distributed dielectric circular rods as wall elements using our originally developed formalism based on the lattice sums technique [3-5]. The latter enables us to calculate the propagation constant of complex modes (namely the phase constant and the attenuation constant) for a wide class of periodic structures and electromagnetic bandgap structures in a very short computation time. The lattice sum approach has been extensively used in modeling the waves scattered and guided by bandgap structures consisting of layered arrays of cylindrical objects, standing in free space or embedded in a dielectric slab, by means of the cylindrical harmonic expansion. In all these cases the Bloch condition and Graf's addition theorem naturally formulate the scattering problem in terms of *lattice sum* coefficients. Hence, there is a considerable number of numerical implementations of scattering problems by periodic cylindrical objects that could immediately benefit from the proposed lattice sum formulation extended to complex phase shifts.

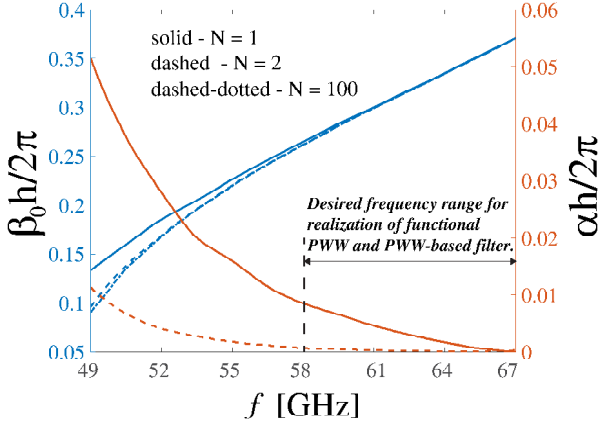


Figure 2. Normalized phase constant $\beta_0 h/2\pi$ (blue line) and normalized attenuation constant $\alpha h/2\pi$ (red line) of the lowest-order TE mode (E_y , H_x , H_z) for a 1-layered (solid line) and 2-layered (dashed line) PWW composed of dielectric rods with: $r = 0.353$ mm, $h = 1.96$ mm, $p = 1.96$ mm, $w=3.92$ mm, $\epsilon=11.56$. The frequency dependence of $\beta_0 h/2\pi$ for a multilayered case where $N = 100$ are also illustrated by a blue dashed-dotted line.

2 Numerical Results and Discussions

We choose a design goal, namely, to realize a functional dielectric PWW and PWW-based passive filter within the frequency range $58 \text{ GHz} < f < 67 \text{ GHz}$. The optimal geometrical parameters for the realization of the functional PWWs in the desired frequency bands can be effectively found based on a combination of our original EM solver (i.e. the full-wave formalism based on the lattice sums technique) and a breeder genetic algorithm [2, 6, 7]. The details regarding the computation time of our method versus other numerical approaches are given in [2]. Our analysis has shown that the dielectric PWW having a width $w = 3.92$ mm, a radius of the dielectric cylindrical posts (as wall elements) of $r = 0.353$ mm, a period of $h = 1.96$ mm, $p = 1.96$ mm and a relative dielectric permittivity of the rods of $\epsilon = 11.56$ (dielectric losses are taken into account using the data published in [8]) can be considered as one of the best candidates for our design goal.

The complex wavenumber $k_{z0} = \beta_0 + i\alpha$, where β_0 and α are phase and attenuation constants in the dielectric PWW are calculated using the lattice sums technique. Figure 2 illustrates the dependence of both the normalized phase constant $\beta_0 h/2\pi$ (blue line) and the normalized attenuation constant $\alpha h/2\pi$ (red line) of the lowest-order mode (E_y , H_x , H_z) for 1-layered (solid line) and 2-layered (dashed line) dielectric PWWs within the frequency range $49 \text{ GHz} < f < 67 \text{ GHz}$. For comparison, the propagation constant of a waveguide structure with $N = 100$ is also shown by the blue dashed-dotted line (the attenuation constant is negligibly small because of the nearly perfect mode confinement). In the desired frequency range $58 \text{ GHz} < f < 67 \text{ GHz}$ for the 2-layered structure, the normalized attenuation constant is

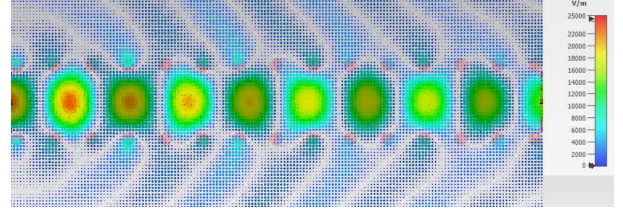


Figure 3. Near field distribution of the electric field E_y of the fundamental mode for a 1-layered dielectric PWW at the operating frequency $f = 62$ GHz.

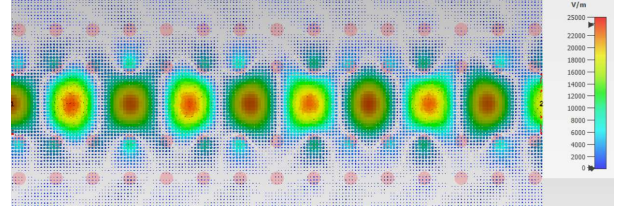


Figure 4. The same as in Fig.1 but for a 2-layered dielectric PWW.

varying between 0.0001- 0.0005, thus the corresponding PWW is applicable to the realization of the functional passive filters.

Furthermore, we have studied near field distributions using CST Microwave Studio. The near field distributions of the electric field E_y of the fundamental mode for a 1- and 2-layered dielectric PWW structure at 62 GHz are depicted in Figs. 3 and 4, respectively. The total length of the structure is $15h$. At this frequency the normalized attenuation constant is $\alpha h/2\pi = 0.0002$. Our numerical analysis has shown a strong field confinement in the case of the 2-layered dielectric PWW, when about 90 % of the injected power is transmitted along the periodic dielectric waveguide structure. As for the 1-layered structure only about 35 % of the initial power can be guided. Our investigations have also shown that the variations of radius, displacement of the layers and the dielectric permittivity of the rods have a substantial effect on the transmittance in the dielectric PWW. The results are illustrated in Figs. 5-7. Thus, the geometrical parameters of the PWW should be properly chosen.

Once the geometrical parameters of the PWW are defined, a bandpass filter is designed by introducing specific arrangements of additional dielectric posts (dielectric losses are taken into account using the data published in [8]) into the waveguide channel. Because of a lack of an efficient technique for the analysis of such kind of dielectric PWW-based filters, we were forced to perform several time-consuming numerical tests by properly selecting the radius, the permittivity and the distance between the elements to design a bandpass filter in the desired frequency range. A schematic view of A dielectric PWW-based filter formed by introducing of five dielectric posts is shown in Fig. 8. Frequency responses of the S-parameters

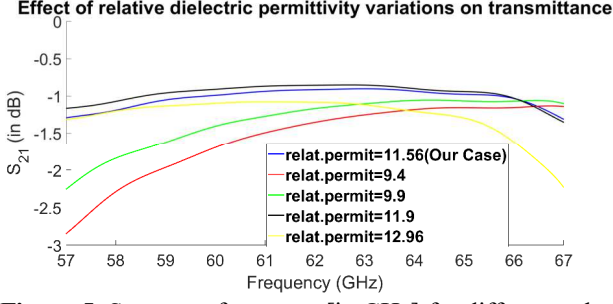


Figure 5. S_{21} versus frequency [in GHz] for different values of a relative dielectric permittivity of the wall elements for a 2-layered ($N=2$) PWW.

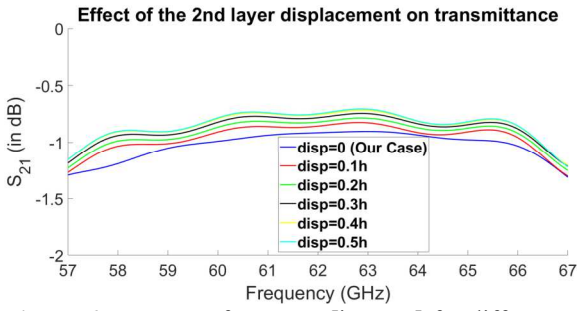


Figure 6. S_{21} versus frequency [in GHz] for different values of a shift of the 2nd layer with respect to the 1st layer for a 2-layered ($N=2$) PWW.

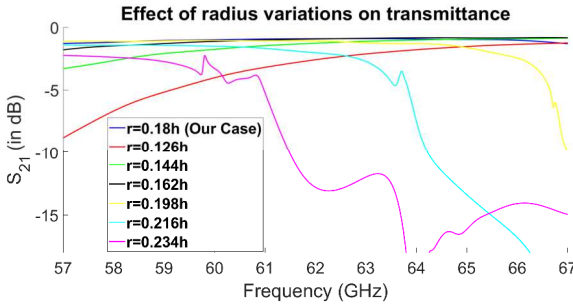


Figure 7. S_{21} versus frequency [in GHz] for different values of a radius of the wall elements for a 2-layered ($N=2$) PWW.

are depicted in Fig. 9 by the solid (S_{21}) and the dashed (S_{11}) curves, respectively. The S-parameters retrieved from CST show a distinct filter behavior from a functional bandpass filter structure based on a dielectric PWW. We succeeded in achieving $S_{11} < -20$ dB in the passband region, however, the bandwidth is slightly larger than we expected [9]. We understand that a better solution could exist. In order to achieve the best filter characteristics in the desired frequency range, a development of a numerically fast full-wave formalism is required. Present research is therefore focusing on the development of an approach, which is directly applicable to our efficient analysis formalism. It is expected to provide a significant speedup over the standard approaches.

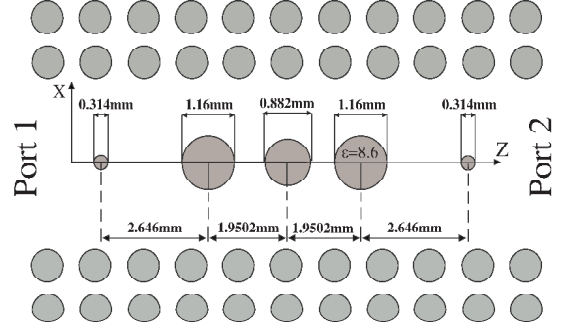


Figure 8. Schematic view of the dielectric PWW-based filter formed by injecting additional dielectric rods into the PWW.

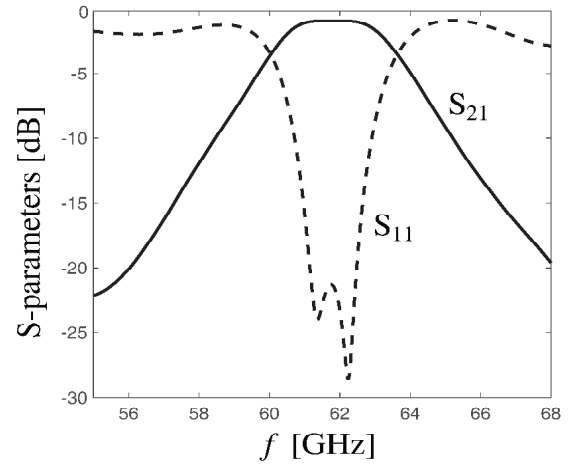


Figure 9. Frequency response of the S-parameters of the dielectric PWW-based filter shown in Fig. 8.

3 Conclusions

In this study we have reported on the numerical investigations of a compact and functional dielectric PWW-based filter, which is potentially applicable also at THz frequencies, where the metallic rods begin to lose their intended properties due to increasing losses. The PWW has been numerically studied and its structural parameters have been properly defined based on our self-contained semi-analytical formalism in combination with a breeder genetic algorithm. Dielectric alternatives to integration concepts are particularly promising especially in the rapidly emerging realm of additively manufactured THz circuits.

4 Acknowledgements

This work was supported by the Deutsche Forschungsgemeinschaft (DFG, German Research Foundation) - TRR 196 MARIE under Grant 287022738 (project M03). The work was supported by Shota Rustaveli National Science Foundation of Georgia (SRNSFG) [grant number: FR-19-4058].

5 References

1. D. Deslandes and K. Wu, "Accurate modeling, wave mechanisms, and design considerations of a substrate integrated waveguide," *IEEE Trans. Microwave Theory Tech.*, vol. 54, no. 6, 2006, 2516-2526.
2. A. Akopian, G. Burduli, V. Jandieri, H. Maeda, W. Hong, A. Omar, K. Yasumoto, D.H. Werner and D. Erni, "Analysis of electromagnetic scattering in post-wall waveguides and its application to optimization of millimeter wave filters," *IEEE Open J. Antennas Propagat.*, Special Section on 'Direct and Inverse Electromagnetic Scattering Methods', vol.1, 2020, 448-455.
3. V. Jandieri, P. Baccarelli, G. Valerio and G. Schettini, "1-D Periodic lattice sums for complex and leaky waves in 2-D structures using higher-order Ewald formulation," *IEEE Trans. Antennas Propag.*, vol. 67, no. 4, 2019, 2364-2378.
4. K. Yasumoto, H. Toyama, and R. Kushta, "Accurate analysis of two-dimensional electromagnetic scattering from multilayered periodic arrays of circular cylinders using lattice sums technique," *IEEE Trans. Antennas Propag.*, vol. 52, no. 10, 2004, 2603-2611.
5. V. Jandieri, P. Baccarelli, G. Valerio, K. Yasumoto and G. Schettini, "Modal propagation in periodic chains of circular rods: real and complex solutions," *IEEE Photonics Technology Letters*, vol. 32, no. 17, 2020, 1053-1056, 2020.
6. Ch. Hafner, J. Smajic, D. Erni, Handbook of Theoretical and Computational Nanotechnology. vol. 8, Michael Rieth, Wolfgang Schommers (Eds.), Chapter 11 "Simulation and Optimization of Composite Doped Metamaterials", pp. 537-613, Stevenson Ranch, CA: American Scientific Publishers, 2006.
7. J. Nagar and D. Werner, "Multiobjective optimization for electromagnetics and optics," *IEEE Antennas Propag. Mag.*, vol. 60, no. 6, 2018, 58-71.
8. J. Baker-Jarvis, M. D. Janezic, B. Riddle, C. L. Holloway, N. G. Paulter, J. E. Blendell, "Dielectric and conductor-loss characterization and measurements on electronic packaging materials," *NIST technical Note*, July, 2001.
9. E. Archemashvili, V. Jandieri, H. Maeda, K. Yasumoto, J. Pistora and D. Erni, "Numerical analysis of dielectric post-wall waveguides and bandpass filters," *Radio Science Letters*, vol. 2, 2021 (in press), doi: 10.46620/20-0027.